PHOTONICS Research

Decaying evolution dynamics of double-pulse mode-locking

Guomei Wang,[1,2,*] Guangwei Chen,[1,2] Wenlei Li,[1,2] Chao Zeng,[1,2] and Huiran Yang[1]

[1]State Key Laboratory of Transient Optics and Photonics, Xi'an Institute of Optics and Precision Mechanics, Chinese Academy of Sciences, Xi'an 710119, China
[2]University of Chinese Academy of Sciences (UCAS), Beijing 100049, China
*Corresponding author: wangguomei@opt.cn

Received 24 April 2018; revised 18 June 2018; accepted 18 June 2018; posted 21 June 2018 (Doc. ID 328885); published 20 July 2018

Taking advantage of the dispersive Fourier transformation technique, the decaying evolution processes of double-pulse mode-locking in a single-walled carbon-nanotube-based Er-doped fiber laser are observed in detail for the first time to our knowledge. The decaying dynamics of the double-pulse mode-locking state is analyzed in the spectral and temporal domains. We reveal that the two pulses in one cluster disappear either simultaneously or one by one during the decaying processes of double-pulse mode-locking states. In addition, the spectral evolution patterns of the special double-pulse states (i.e., bound states) are extremely distinct at different decline rates of the pump power.

OCIS codes: (320.7120) Ultrafast phenomena; (140.3500) Lasers, erbium; (140.4050) Mode-locked lasers; (140.3510) Lasers, fiber.

https://doi.org/10.1364/PRJ.6.000825

1. INTRODUCTION

Fiber lasers possess inherent advantages of having high efficiency, being alignment-free, and having excellent beam quality [1,2], and thus have many applications in materials processing, fiber optic communications, optical frequency combs, etc. Due to the limitation of effective gain bandwidth, the gain can no longer amplify a very narrow pulse but imposes an extra loss on it, which results in the pulse splitting into two pulses with broader pulse widths [3]. Independent of the concrete mode-locking techniques, passive mode-locking can easily run into the multipulse state under strong pumping strength, especially the double-pulse state, which has been widely observed in various platforms, such as ion-implanted semiconductor saturable absorber mirror mode-locked Ti:sapphire lasers [4], Kerr lens mode-locked Ti:sapphire lasers [5], and nonlinear polarization rotation mode-locked fiber laser [6]. According to previous reports, it has been confirmed that multipulse clusters can realize many interesting optical interactions, including soliton rain, bunched solitons, and soliton molecules [7–9]. However, most of the time, the multipulse state is still a very unwanted phenomenon in many applications of the stable mode-locked lasers due to the smaller pulse energy and broader pulse width [3]. Therefore, in order to further improve the performance of fiber lasers, it is essential to reveal the underlying principle of the multipulse state.

Because the conventional spectrometers scan relatively slowly, they provide time-averaged data over many consecutive pulses and do not permit real-time measurements. Many transition evolution phenomena about the double-pulse mode-locking escape from being studied experimentally. Recently, a powerful method—the dispersive Fourier-transform (DFT) technique—has attracted the extensive attention of numerous researchers [10,11]. In the DFT, analogous to spatial far-field diffraction, the intensity profile of the pulse will match its spectral envelope when the pulse is injected into a high-dispersion element and stretched ultimately [12]. Because the stretched waveform is slow enough to be within the bandwidth of a real-time digitizer, it is possible to directly measure a series of single-shot spectra at the full laser repetition rate [13]. With its unique ability to perform ultrafast real-time spectroscopic measurements, the DFT technique has been employed for a diverse range of sensing and detecting applications. Liu *et al.* have studied the dissipative rogue waves in an ultrafast fiber laser by using the all-optical DFT [14]. Wong *et al.* have investigated the multipulse dynamics and the collision-induced soliton self-reshaping process in the standard passively mode-locked fiber lasers [15,16]. Based on simultaneous DFT and time-lens measurements, Ryczkowski *et al.* have characterized the spectral and temporal evolution of ultrashort dissipative solitons [17]. Apart from the achievements mentioned above, there is much other significant progress in real-time measurements by using DFT [18–21]. However, the decaying evolutions of double-pulse mode-locking still escape from direct experimental observation.

In this paper, we use the real-time DFT technique to analyze the decaying evolution of double-pulse mode-locking states in an Er-doped fiber (EDF) laser. The spectral width and pulse

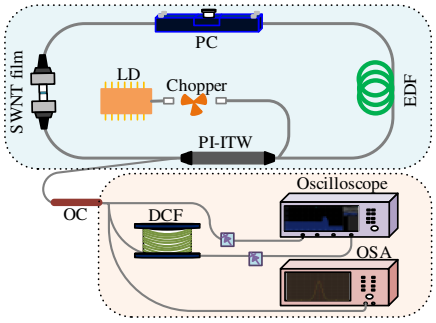

Fig. 1. Setup of the fiber laser and the measurement system.

energy of individual pulses are carefully studied at high temporal and spectral resolution. During the decaying processes of double-pulse mode-locking, there are two different evolutionary forms of both pulses: disappearing simultaneously or one by one. In addition, the spectral evolution patterns of the special double-pulse states (i.e., bound states) at different decline rates of the pump power are revealed in detail. We believe that our results will broaden the horizons of multipulse mode-locking.

2. EXPERIMENTAL SETUP

The experimental configuration is shown in Fig. 1, which is comprised of a fiber laser and the observation system. A single-walled carbon nanotube (SWNT)-based passively mode-locked EDF laser is investigated. It consists of a 4.1-m EDF, a polarization controller (PC), a mode-locker (i.e., a piece of home-made SWNT film with a recovery time of about 1 ps and sandwiched by two fiber connectors), a ~3.81-m-long pigtailed single-mode fiber (SMF), and a polarization-independent hybrid combiner of an isolator, a tap coupler, and a wavelength division multiplexer (PI-ITW). The PI-ITW is used to ensure unidirectional operation, extract intracavity power with ratio of 10% from the ring laser cavity, and input the pump power from a 980-nm laser diode (LD). An optical chopper is placed in the free-space section between the LD and PI-ITW as an on–off switch of the pump power. Dispersion parameters of the EDF and SMF are about −9 and 17 ps/(nm · km), respectively, and therefore the net dispersion of this fiber laser is calculated as −0.036 ps^2. The output power is split into three branches through a 60:20:20 optical coupler (OC) for spectral-temporal analysis. The observation system used in Fig. 1 mainly consists of a 5-km-long dispersion-compensating fiber (DCF), a 4-GHz, 20-GSa/s real-time oscilloscope, two high-speed 6-GHz photodetectors (PDs), and an optical spectrum analyzer (OSA). The DCF provides a total accumulated dispersion of ~940 ps^2, and the spectral resolution of our DFT configuration is about 0.34 nm, which allows the shot-to-shot spectra to be recorded in detail by the oscilloscope.

3. EXPERIMENTAL RESULTS AND DISCUSSION

When the pump power is increased to 8.5 mW, single-pulse mode-locked operation can be easily achieved owing to the saturable absorption of the SWNT film. Increasing the pump power to ~13.8 mW, the state evolves into double-pulse mode-locking state. Tuning the PC carefully, a stable double-pulse mode-locking state is achieved in the laser cavity at the pump power of ~17.7 mW. In this stable state, the energy of the output pulse is calculated as ~7.15 pJ. As shown in Fig. 2(a), the interval between the pulse clusters is ~38.5 ns, which corresponds to a fundamental repetition rate of 26 MHz. The temporal series, which brings the spectral information of each pulse acquired by the DFT, is displayed in Fig. 2(b). When the pulse propagates through the 5-km DCF, its width at half-maximum is stretched to ~4 ns from ~720 fs. Since the interval between the pulses in one cluster is about 14.1 ns, no overlap appears between the stretched pulses. The single-shot spectra of both two pulses (green curve) are exhibited in Fig. 2(c). Slight fluctuations can be seen in this single-shot spectral curve, which results from the digitization of the fast oscilloscope in DFT measurements. Owing to the weak intensity of the spectral sideband and the slight fluctuations mentioned above, the Kelly sidebands are not exhibited on the spectra obtained by the DFT technique. The average spectrum of each pulse calculated from 100 single-shot spectra (blue curve) agrees well with the averaged spectrum directly obtained by the OSA, as revealed in Fig. 2(c). Due to the weak pulse peak intensity, the effect of self-phase modulation in the DCF can be neglected [22]. Obviously, in the stable double-pulse mode-locking state, the two pulses in one cluster have almost the same spectrum, with a spectral width of ~5.3 nm and center wavelength of ~1561.7 nm. The time-bandwidth product is 0.47, indicating that the pulses are slightly chirped.

When the chopper shades the pump power, the stable double-pulse mode-locking state decays gradually, and both the temporal and spectral domains' information is captured. The recorded data can thus cover the entire decaying evolution of the double-pulse mode-locking, i.e., from stable state to annihilation. A two-dimensional evolution diagram can be built by segmenting the time series into intervals of length (i.e., 38.5 ns), whose vertical axis depicts the dynamics across

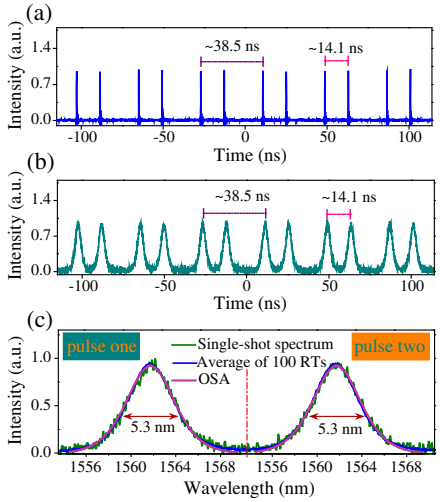

Fig. 2. (a) Typical oscilloscope trace; (b) corresponding stretched pulses captured by DFT; (c) single-shot spectrum, average spectrum calculated from 100 single-shot spectra, and spectrum recorded by OSA.

consecutive round-trips, and the horizontal axis exhibits the information within a single round-trip. The spectral evolution process of both pulses is shown in Fig. 3(a), which contains 25,000 consecutive round-trips. As revealed in this figure, the center wavelengths of both pulses are about 1561.7 nm. Before the decrease of pump power, the spectral width remains constant at about 5.3 nm. Accompanied by the decay of the pump power, the spectral width diminishes by degrees to zero, as exhibited in Fig. 3(c). It is worth noting that, no matter whether in the stable state or the decaying process, the spectral widths of both pulses always remain identical. Moreover, the interval between both pulses in one cluster remains at ~14.1 ns during the whole evolution process, as presented in Fig. 3(b). For the energy quantization theory, a natural consequence of the gain competition between the solitons, the two pulses possess the same pulse energy at the stable double-pulse mode-locking state [23], as revealed in Figs. 3(b) and 3(c). Furthermore, the variation trends of pulse energy and the spectral width are almost identical during this evolution process, as displayed in Fig. 3(c).

Another stable double-pulse mode-locking state with a spectral width of ~5 nm and interval between both pulses of ~13.2 ns is acquired by properly tuning the PC when the pump power is maintained unchanged. The diverse intervals of different stable double-pulse mode-locking states may be caused by the gain-recovery mechanism [24]. Different from the evolution process shown in Fig. 3, during which both pulses disappear synchronously, the two pulses shown in Fig. 4 disappear in the laser cavity one by one. This phenomenon is mainly attributed to the combination of gain competition, positive feedback, and energy balance [25]. The spectral evolution of this process is presented in Fig. 4(a), and the spectral width of each pulse is about 5 nm at the stable mode-locking state. In order to recognize the spectral width evolution dynamics of each pulse in detail, the transformation curves are shown in Fig. 4(c). The spectral widths of both pulses remain identical and decrease simultaneously in most of the decaying process.

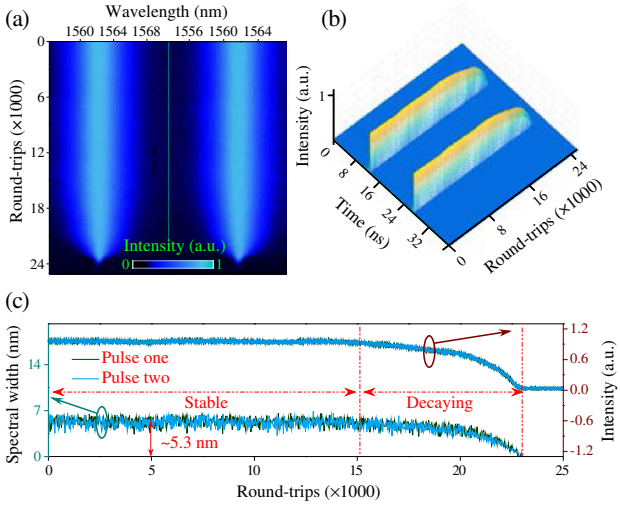

Fig. 3. (a) Spectral evolution of both pulses; (b) temporal behavior during the evolution process; (c) changing of the energy and spectral width of both pulses.

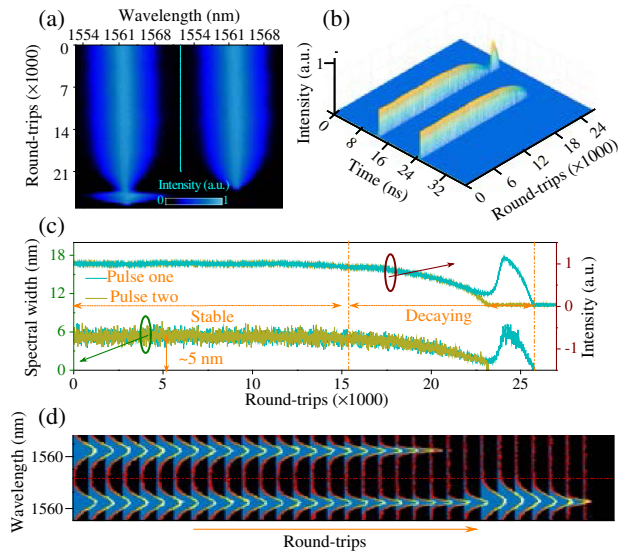

Fig. 4. (a) Spectral evolution of both pulses; (b) temporal behavior during the evolution process; (c) changing of the energy and spectral width of both pulses; (d) the zoom-in waterfall plot of the spectral pattern extracted from the dataset in (a).

At about the 23,200th round-trip, the spectral width of one pulse decreases to zero, and the spectral width of the other pulse begins to increase at the same time. As shown in Figs. 4(a) and 4(c), the spectral width of the remaining pulse raises up to ~5.5 nm, even larger than that of the stable mode-locking state. With the decrease of pump power, the spectral width drastically dwindles in the following round-trips. To directly observe the single-shot spectral dynamics in the decaying evolution stage, the zoom-in waterfall plot of each pulse's spectral pattern is provided as an example in Fig. 4(d). It contains 31 single-shot spectra, which are extracted from the 17,500th to the 26,500th round-trip of Fig. 4(a) uniformly. There are three intriguing features presented in the spectral evolution patterns that mark the decaying process signature: the different transformations of both pulses' spectra, a dynamic redshift (about 1 nm) of the remaining pulse during the vanishing of the other pulse, and spectral broadening of the remaining pulse. In order to analyze the temporal transformation information of both pulses, a three-dimensional graph is displayed in Fig. 4(b). Similar to the process depicted in Fig. 3(b), the pulse energy and the interval between two pulses remain constant at the stable state. However, the two pulses do not disappear simultaneously. The remaining pulse gradually becomes stronger first and then weakens to annihilation. Along with the decrease of the pump power, the double-pulse mode-locking state converts into single-pulse state at the pump power of ~11.26 mW. Since the remaining pulse exists in the cavity for about 2600 round-trips, and the decline rate of the pump power is about 1.36 μW/round-trip (i.e., 35.39 μW/μs), it indicates that the remaining pulse dies away at a pump power of ~7.72 mW. Evidently, pump powers of 7.72 and 11.26 mW are lower than that of the start of mode-locking (8.5 mW) and the double-pulse state (13.8 mW), respectively, which is the typical pump hysteresis effect of the soliton operation [3].

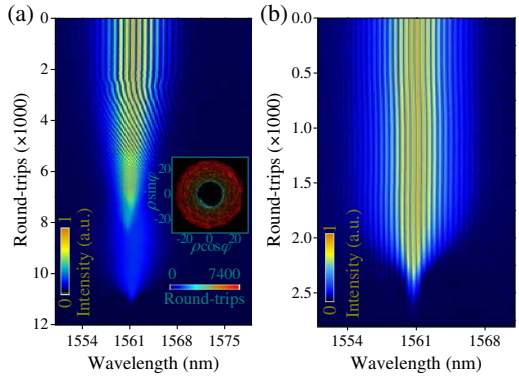

Fig. 5. Spectral evolution of the bound state at the decline rate of pump power of (a) ~1.09 μW/round-trip and (b) ~11.32 μW/round-trip. Inset of (a): decaying dynamics of the bound state mapped in the interaction plane.

The interaction between slightly overlapping pulses could lead to the formation of bound state with a fixed time separation [26]. By properly adjusting the PC, a stable bound-state operation can be achieved in the laser cavity. The stable spectral modulation period is about 0.92 nm, which corresponds to the temporal separation (ρ) of ~8.84 ps. When the pump power is decreased to zero by the decline rate of ~1.09 μW/round-trip, the spectral evolution process is shown in Fig. 5(a). According to the spectral evolution, it can be seen that the two bound pulses depart away from each other gradually with a complex change of relative phase (φ). The modulation depth of the bound-state spectrum decreases slowly along with the number of round-trips, indicating that one of the two bound pulses is becoming weaker and weaker [26]. At about the ~7500th round-trip, the weaker pulse vanishes, and the bound state turns into single-pulse state. Owing to the continuous decline of the pump power, the spectrum becomes narrower, and the remaining pulse finally disappears in the laser cavity. As shown in the right inset of Fig. 5(a), the evolution of the bound-state configuration space during the transition is visualized by an interaction plane ($\rho \cdot \sin\varphi$ and $\rho \cdot \cos\varphi$), whose radius and angle correspond to the temporal separation and relative phase between two bound pulses, respectively [27]. Over 7400 round-trips of bound states prior to the disappearance of the weaker pulse are presented in the interaction plane, and complex changes of temporal separation and relative phase between two bound pulses are illustrated in the trajectories. When the decline rate of the pump power is ~11.32 μW/round-trip, the spectral evolution of another stable bound state is displayed in Fig. 5(b). Due to the sharp decline of pump power, the spectra become narrower quickly without any changes of the spectral modulation period, as shown in Fig. 5(b). This suggests that the temporal separation and relative phase between two bound pulses remain constant during the decaying process. In addition, the number of round-trips of the transition process (from stable state to annihilation) is about 1000, which is much smaller than that shown in Fig. 5(a). The difference between the two evolutionary processes mainly depends on whether there are effective perturbations when the pulse energy drops to a critical value [25].

4. CONCLUSION

In summary, we experimentally investigated the decaying dynamics of double-pulse mode-locking states in an SWNT-based fiber laser by the DFT technique. The decaying dynamics are analyzed in both the spectral and temporal domains. We reveal that the transformation trends of spectral width and pulse energy along the round-trips during the decaying processes are very analogous. The two pulses in one cluster disappear either simultaneously or one by one during the decaying processes of the double-pulse mode-locking state. At different decline rates of the pump power, the evolution patterns of the bound states are extremely distinct in the temporal separation and relative phase. The obtained results could pave the way for further investigation of the complex soliton dynamics in nonlinear optical systems, which could also be helpful for the communities dealing with fiber lasers.

Funding. National Natural Science Foundation of China (NSFC) (61223007).

REFERENCES

1. P. Grelu and N. Akhmediev, "Dissipative solitons for mode-locked lasers," Nat. Photonics **6**, 84–92 (2012).
2. D. Mao, X. Q. Cui, W. D. Zhang, M. K. Li, T. X. Feng, B. B. Du, H. Lu, and J. L. Zhao, "Q-switched fiber laser based on saturable absorption of ferroferric-oxide nanoparticles," Photon. Res. **5**, 52–56 (2017).
3. D. Y. Tang, L. M. Zhao, B. Zhao, and A. Q. Liu, "Mechanism of multi-soliton formation and soliton energy quantization in passively mode-locked fiber lasers," Phys. Rev. A **72**, 043816 (2005).
4. M. J. Lederer, B. Luther-Davies, H. H. Tan, C. Jagadish, N. N. Akhmediev, and J. M. Soto-Crespo, "Multipulse operation of a Ti:sapphire laser mode locked by an ion-implanted semiconductor saturable-absorber mirror," J. Opt. Soc. Am. B **16**, 895–904 (1999).
5. C. Spielmann, P. F. Curley, T. Brabec, and F. Krausz, "Ultrabroadband femtosecond lasers," IEEE J. Quantum Electron. **30**, 1100–1114 (1994).
6. A. Komarov, H. Leblond, and F. Sanchez, "Passive harmonic mode-locking in a fiber laser with nonlinear polarization rotation," Opt. Commun. **267**, 162–169 (2006).
7. S. Chouli and P. Grelu, "Rains of solitons in a fiber laser," Opt. Express **17**, 11776–11781 (2009).
8. B. Grudinin and S. Gray, "Passive harmonic mode locking in soliton fiber lasers," J. Opt. Soc. Am. B **14**, 144–154 (1997).
9. P. Grelu, F. Belhache, F. Gutty, and J. M. Soto-Crespo, "Phase-locked soliton pairs in a stretched-pulse fiber laser," Opt. Lett. **27**, 966–968 (2002).
10. D. R. Solli, J. Chou, and B. Jalali, "Amplified wavelength–time transformation for real-time spectroscopy," Nat. Photonics **2**, 48–51 (2008).
11. R. Salem, M. A. Foster, and A. L. Gaeta, "Application of space-time duality to ultrahigh-speed optical signal processing," Adv. Opt. Photon. **5**, 274–317 (2013).
12. K. Goda and B. Jalali, "Dispersive Fourier transformation for fast continuous single-shot measurements," Nat. Photonics **7**, 102–112 (2013).
13. P. V. Kelkar, F. Coppinger, A. S. Bhushan, and B. Jalali, "Time-domain optical sensing," Electron. Lett. **35**, 1661–1662 (1999).
14. M. Liu, A. P. Luo, W. C. Xu, and Z. C. Luo, "Dissipative rogue waves induced by soliton explosions in an ultrafast fiber laser," Opt. Lett. **41**, 3912–3915 (2016).
15. Y. Yu, B. W. Li, X. M. Wei, Y. Q. Xu, K. K. M. Tsia, and K. K. Y. Wong, "Spectral-temporal dynamics of multipulse mode-locking," Appl. Phys. Lett. **110**, 201107 (2017).

16. Y. Wei, B. W. Li, X. M. Wei, Y. Yu, and K. K. Y. Wong, "Ultrafast spectral dynamics of dual-color-soliton intracavity collision in a mode-locked fiber laser," Appl. Phys. Lett. **112**, 081104 (2018).
17. P. Ryczkowski, M. Närhi, C. Billet, J. M. Merolla, G. Genty, and J. M. Dudley, "Real-time full-field characterization of transient dissipative soliton dynamics in a mode-locked laser," Nat. Photonics **12**, 221–227 (2018).
18. H. J. Chen, M. Liu, J. Yao, S. Hu, J. B. He, A. P. Luo, W. C. Xu, and Z. C. Luo, "Buildup dynamics of dissipative soliton in an ultrafast fiber laser with net-normal dispersion," Opt. Express **26**, 2972–2982 (2018).
19. F. Runge, N. G. Broderick, and M. Erkintalo, "Dynamics of soliton explosions in passively mode-locked fiber lasers," J. Opt. Soc. Am. B **33**, 46–53 (2016).
20. C. Lecaplain and P. Grelu, "Rogue waves among noiselike-pulse laser emission: an experimental investigation," Phys. Rev. A **90**, 013805 (2014).
21. F. G. Runge, N. G. R. Broderick, and M. Erkintalo, "Observation of soliton explosions in a passively mode-locked fiber laser," Optica **2**, 36–39 (2015).
22. G. P. Agrawal, *Nonlinear Fiber Optics* (Academic, 2007).
23. B. Grudinin, D. J. Richardson, and D. N. Payne, "Energy quantisation in figure eight fibre laser," Electron. Lett. **28**, 67–68 (1992).
24. J. N. Kutz, B. C. Collings, K. Bergman, and W. H. Knox, "Stabilized pulse spacing in soliton lasers due to gain depletion and recovery," IEEE J. Quantum Electron. **34**, 1749–1757 (1998).
25. A. Komarov, H. Leblond, and F. Sanchez, "Multistability and hysteresis phenomena in passively mode-locked fiber lasers," Phys. Rev. A **71**, 053809 (2005).
26. M. Grapinet and P. Grelu, "Vibrating soliton pairs in a mode-locked laser cavity," Opt. Lett. **31**, 2115–2117 (2006).
27. N. N. Akhmediev, A. Ankiewicz, and J. M. Soto-Crespo, "Multisoliton solutions of the complex Ginzburg-Landau equation," Phys. Rev. Lett. **79**, 4047–4051 (1997).